AIAA JOURNAL
Vol. 39, No. 11, November 2001

Fast-Response Cylindrical Air Bearing Balance

John C. Magill,* Michael F. Hinds,† and Mark R. Malonson‡
Physical Sciences, Inc., Andover, Massachusetts 01810-1044

The air bearing balance described has been designed to support the dynamic force measurement requirements of virtual flight testing. This balance is a single-degree-of-freedom air bearing spindle. The bearing gas film is instrumented with fast-response pressure sensors that enable the determination of forces and moments. The device thus permits the measurement of unsteady aerodynamic loads on spinning test articles. The balance also incorporates a supply of high-pressure air, delivered to the model without friction, for pneumatic actuators or reaction control jets. Spin at up to 20,000 rpm is made possible with a brushless motor. The focus is on calibration properties of the balance, particularly the influence of rotation angle and spin rate on the calibration parameters. Combined linearity and repeatability errors less than 0.5% full scale are achieved at a fixed angle. Spin rate and angle deviations introduce calibration variations as large as 20%, but angle and speed curve fitting are shown to reduce this error to less than 1.5%.

Introduction

THIS paper describes the development and testing of a cylindrical air bearing balance. The balance is intended for use in testing spinning projectile or missile models, as well as for making measurements on aircraft models mounted free to roll.

Air bearing balances are being developed to facilitate dynamic testing in wind tunnels, such as virtual flight testing.[1] Dynamic wind-tunnel testing requires the ability to measure unsteady loads on test models as they undergo rapid maneuvering motions. When dynamic stability data are obtained or control system performance is evaluated, it is often unacceptable to interfere with the natural motion of the vehicle by adding artificial damping. Conventional ball- or roller-bearing pivots introduce friction and, hence, damping to the motion that is not present in flight.

To circumvent the false damping problems, the devices described here use air bearings[2–7] to provide frictionless motion. An air bearing consists of two surfaces, one free or floating and one fixed (see Fig. 1). The surfaces are separated by a thin film of air that is injected through orifices in the fixed surface, much like the operation of an air hockey table. Typical film thicknesses are between 12 and 25 μm (0.0005 and 0.001 in.). Because there is no contact between the surfaces, there is very little friction when the floating element moves parallel to the fixed surface.

All of the load on the floating element, due to gravity, aerodynamic forces, or inertial loads, is supported by the pressure of the air film. If a load is applied to the floating element pushing it toward the fixed surface, the film gets locally thinner. This increases the film flow resistance and, thus, decreases film air mass flow. At the reduced mass flow, the pressure drop from the air supply through the injection orifice is smaller, resulting in higher film pressures. This higher pressure works against the applied load. Similar arguments are made to show how the bearing surfaces can support moment loads. The result is a thin film that acts as a distributed spring.[4]

Because the loads are supported by the film pressure, measurements of the film pressure can be used to determine the loads applied to the floating element. This load sensing concept is known as an air bearing balance. A typical sensor placement is shown in Fig. 1a. If bearing surfaces are arranged to oppose one another (Fig. 1b), the difference in pressure between the two surfaces can be used to determine loads because the mean pressures are balanced on opposing surfaces. The load sensitivity is then independent of the mean film pressure and is determined by the sensitivity of the differential pressure sensor. Because the mean pressure determines the stiffness of the air film spring, there is no tradeoff between sensitivity and stiffness, a key advantage over strain measurement balances.

The air bearing wind-tunnel balance concept was originally explored by Haldeman and Weinberg.[8] They constructed a cylindrical journal-and-thrust bearing to make measurements on rotating, ablating models in a wind tunnel. Their design included pressure taps on the bearing surfaces to measure gas film pressures and, in turn, determine loads on the balance. The pressure taps were connected via tubes to pressure transducers located outside of the wind tunnel. The deficiency in their balance was its frequency response. Because long tubes had to be connected from the pressure taps to the sensors, high-frequency load measurements could not be made. In fact, it took approximately 7 s for their measurements to reach a steady state. Micromachined fast-response pressure sensors are now available that can be installed inside of the gas bearing,[9,10] so that no long tubes are required.

This paper focuses on design, test, and calibration experience with a cylindrical bearing. Repeatability and accuracy are addressed. Particular attention is paid to calibration of the spinning bearing because spin rate alters the balance sensitivity. The following paragraphs describe the construction of the device and its instrumentation subsystems. The ensuing sections will describe the static calibration and spin testing processes, as well as the results from both test series.

Cylindrical Balance Design

The bearing is configured as shown in Fig. 2. It consists of a pair of journal bearings and a thrust bearing. The outer element is the floating or moving element. The inner element is fixed, typically attached to the end of the sting in a wind tunnel. The bearing is capable of rotating about a single axis and is, thus, designated a one-degree-of-freedom (1-DOF) device. Figure 3 shows the mechanical details in a cross-sectional view of the device.

The journal bearings consist of concentric cylinders, separated by a gap 18 μm (0.00075 in.) thick. Each journal bearing incorporates of a pair of injection orifice rows. The journal bearings are separated by sufficient distance to permit them to carry moments about the journal's transverse axes. The journal bearing is 50.8 mm (2.0 in.) in diameter and is capable of supporting radial loads up to 2850 N (640 lb).

The thrust bearing is double-acting (composed of opposing faces), enabling both thrust and drag loads to be supported. The thrust bearing faces are annular. Loads up to 670 N (150 lb) can be supported by the thrust bearing.

The air bearing balance was machined from 17-4 PH stainless steel. All surfaces that face the bearing film were coated with an electroless nickel/Teflon® film. The surface treatment provides a hard, low-friction surface to prevent surface scratching and galling during setup and handling.

Received 11 March 2000; revision received 19 January 2001; accepted for publication 16 May 2001.

*Principal Research Engineer, 20 New England Business Center. Member AIAA.
†Senior Programmer, 20 New England Business Center.
‡Senior Research Engineer, 20 New England Business Center.

A tube from the sting support carries the auxiliary air to a plenum at the far end of the thrust bearing. We chose a tube with a 6.4 mm ($\frac{1}{4}$ in.) o.d. and 4.8 mm ($\frac{3}{16}$ in.) i.d. to carry this flow. This is the largest tube that can fit through the journal bearing sensor cartridges and through the center of the thrust bearing. Flow rate calculations using adiabatic compressible flow relations show that such a tube can carry 0.37 kg/s (0.81 lbm/s) of air without choking. However, the pressure drop at that flow rate would be 800 kPa (1200 psi) from the source to the plenum, which is unacceptable. Assuming we want the pressure drop between the source and the plenum to be no more than 10% (1.2 MPa/1800 psi in plenum), the maximum flow rate through the supply tube is about 0.18 kg/s (0.4 lbm/s).

The stationary supply tube must feed a rotating plenum, without adding any friction to the rotating bearing or any axial loads to the bearing that would add an error to the thrust load measurement. To accomplish this, we used a double near seal approach (Fig. 4). The supply tube protrudes from the thrust bearing disk into a cavity within the plenum. A near seal is formed by a sharp-edged hole in each wall of the cavity that closely surrounds the supply tube at both ends of the cavity. The double near seal is necessary because the supply tube must not terminate inside the high-pressure supply cavity. Otherwise, a large thrust load is produced. Air enters the supply tube through a pair of opposing holes on the sides of the tube so that no net force is produced by the auxiliary airflow. Holes in the cavity feed air to the plenum. The double near seal allows a small amount of air to leak equally out both ends of the cavity, thereby avoiding any contact load between the supply tube and the plenum. Notice that every surface exposed to a high pressure is balanced by an opposing surface and that all air is fed through opposing radial holes, so that no net load results from the auxiliary air system. The leaking air is vented into the interior of the journal along with the vented air from the bearing injection ports.

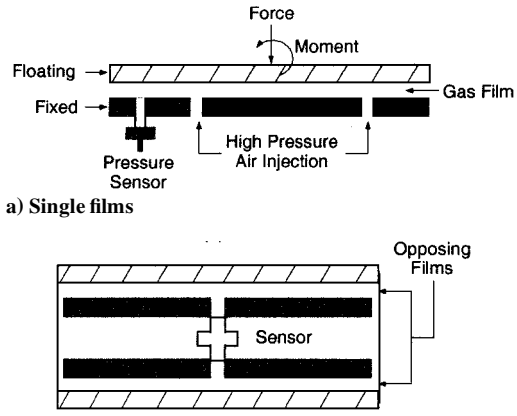

Fig. 1 Air bearing balance concept.

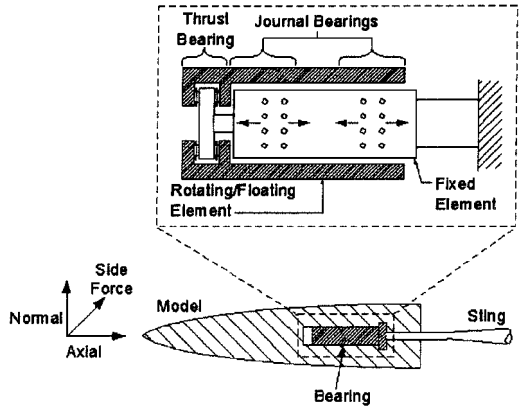

Fig. 2 Air bearing balance configuration and model placement (1-DOF).

Spin Motor

Spin is imparted to the floating element by a 12-pole brushless motor. The motor as purchased is frameless and contains no bearings. Rather, it utilizes the air bearings. The motor is capable of spin rates up to 20,000 rpm and torques up to 2.7 N · m (24 in. · lb).

An inductive power sensor measures the electrical power consumed by the motor. Dividing power by speed yields motor torque. This assumes that the motor is perfectly efficient at converting electrical power to mechanical. If the motor efficiency is known, this discrepancy can be easily corrected.

An optical quadrature encoder was installed next to the motor to measure the angular position of the rotating element. The encoder provides 4000 counts per revolution of the bearing. The encoder outputs are converted to position by an encoder interface board in the instrumentation module computer.

Instrumentation

As shown in Fig. 5, five micromachined sensors are used to measure film pressures and, hence, bearing loads. Each sensor is about 13 mm in diameter and 13 mm long and contains a diaphragm instrumented with a full strain gauge bridge. A 25 × 13 mm board

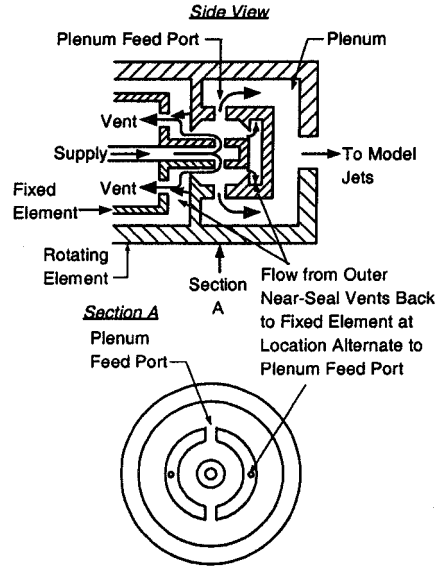

Fig. 4 Auxiliary airflow system.

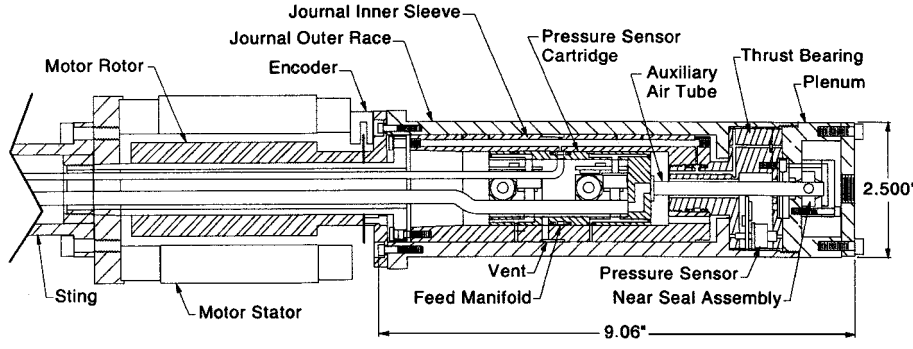

Fig. 3 Air bearing balance mechanical details (1-DOF).

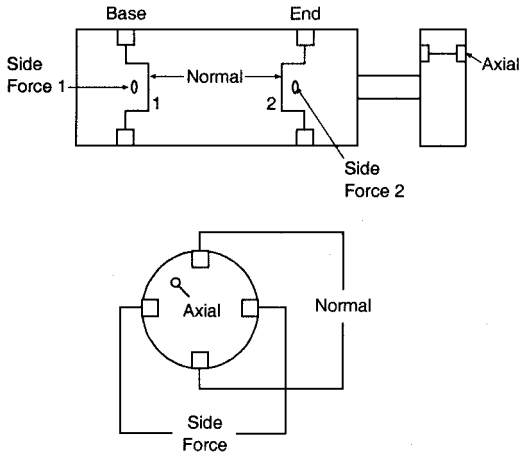

Fig. 5 Placement of sensor for five-component load sensing.

was added at the base of the device and provides a current source and signal amplifier for the sensor. The sensors have a time constant less than 1 ms.

Each journal bearing contains a pair of sensors, one oriented vertically and one horizontally. In principle, they measure the vertical and horizontal forces at two locations. The sum of vertical loads at the two journal bearings is the total normal force, and the difference in vertical loads is the pitching moment. Similarly, the horizontal sensors can be used to sense side force and yawing moment. A single sensor measures the difference in pressure across the thrust bearing, allowing the determination of axial force.

Though the preceding paragraph describes a clear and independent sensing scheme, the data reduction procedure must account for deviations from this idealization. All of the sensors react to loads in other than their principal directions. These off-axis influences are measured in the calibration process as described in the later section, "Calibration Procedure."

Because of the density of instrumentation components within the journal, assembly was one of the most challenging aspects of the development effort. To facilitate assembly, all of the sensors were first installed in a cylindrical cartridge, which also contains the feed manifold that supplies air to the bearings. Sections of the cartridge wall can be removed, enabling installation of the sensors. Once assembled, the cartridge is inserted into the bearing. Elastomer O-rings on the outer surface of the cartridge form a sealed passage between sensors and the bearing pressure taps.

Though the air bearing is axisymmetric, the current balance is more sensitive in the horizontal direction than the vertical. The horizontal sensors have a full span differential pressure range of 15 psi (101 kPa), whereas the vertical sensors have a 50-psi (345-kPa) range. The sensitivities can be changed by replacing the sensors, without making any changes to the bearing itself.

A 233-MHz Pentium processor in the instrumentation module controls acquisition, applies calibrations to measured signals to compute loads, and sends force and moment measurements out of D/A ports. Before acquisition, all pressure sensor signals are low-pass filtered with fourth-order Butterworth filters with a cutoff frequency of 1 kHz. The Pentium can compute loads from signals at up to 2 kHz. The instrumentation module also includes an interface to the bearing optical encoder, which measures the rotor angle.

Facilities and Procedures

Static Calibration Rig

Calibration loads were applied in the Physical Sciences, Inc. (PSI), Air Bearing Balance Calibration Facility (Fig. 6). This apparatus provides controlled supplies of air for the bearing and its auxiliary air system and performs automated loading necessary for static calibration of the load sensors. The frame is constructed from extruded aluminum beams. The entire assembly is encased in 12.5-mm Lexan™ to contain components in the event of a failure during a high-speed spin test.

A set of five pneumatic cylinders apply loads for calibration. A precision load cell is located in series with each actuator to provide

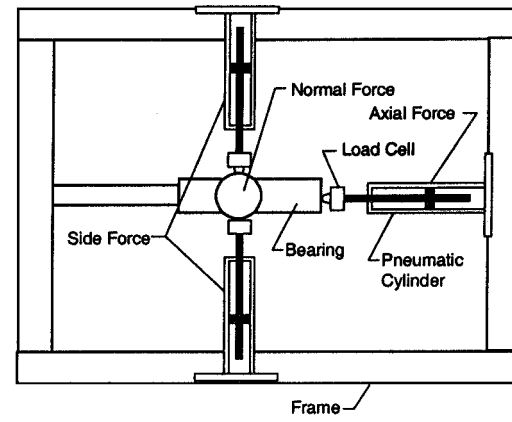

Fig. 6 Calibration rig.

a National Institute of Standards and Testing traceable calibration reference. Computer-controlled valves connect the cylinders to their air supply, so that the loading procedure can be automated. The cylinders can be moved along the support beams to change the load center or to apply moment loads.

A calibration body is installed on the bearing during the calibration process. This steel cylinder attaches to the bearing at the same points that would secure a wind-tunnel model. This ensures that calibration loads are transmitted to the bearing exactly as the loads expected in a wind-tunnel test.

Calibration Procedure

The calibration procedure is automated with the aid of a personal-computer-type computer. A schedule of loads for each axis is prescribed to the calibration program. For each point, the computer opens the cylinder supply valves until the prescribed load is approximately achieved. The computer then waits a preselected settling period before beginning data acquisition. Then, a set of samples from all load cells and bearing pressures is measured and stored for later reduction. In this way, a large number of test loads can be applied automatically. For the results presented here, the settling time was 20 s. Signals were then acquired for 20 s at 5 Hz and averaged.

Because of imperfections in machining, the calibration for an air bearing balance varies with rotor angle. Thus, the calibration must be performed at several angles. For the results presented later in this paper, the calibration was repeated every 45 deg of rotor position.

Spin Testing

The purpose of performing spin calibration tests was to quantify the impact of spin-induced hydrodynamic effects on the calibration parameters. There are two primary mechanisms by which spin changes the relationship between pressures applied and measured at the taps.

The flow in the journal bearings is primarily axial in the absence of spin motion. When the bearing is spinning, a circumferential velocity is imposed on the film. The circumferential velocity component at 20-krpm spin rate is about 10% of the axial velocity in the film. When a load is applied to the bearing, the fixed and floating elements are eccentric, so that the film height varies around the bearing. As the flow is forced around the bearing, the fluid is forced into a narrower passage on one side of the bearing and permitted to expand on the opposite side, causing additional pressure variation across the bearing when compared to the nonrotating case. This is, in fact, the source of load carrying capacity in hydrodynamic (self-acting) fluid film bearings. This change in the bearing pressure distribution will alter the measured pressure at the taps for a particular load and must, thus, be considered in the bearing calibration.

Even at lower speeds, where circumferential velocities are small compared with the axial velocities, dynamic film effects can be induced by the spin. As will be demonstrated by the static calibration data later in this paper, the film properties vary with the angle of the rotor due to manufacturing imperfections. As the bearing spins, the film experiences a time-varying height at any particular local station. This can produce a squeeze effect on the film. Depending on the relative rate of motion of the two surfaces, the squeeze film

effects can provide damping, or they can add stiffness to the film. The squeeze film behavior is, thus, speed dependent, and its impact on the film pressures must be quantified.

The spin calibration procedure described hereafter will quantify both of the spin effects just described. It does not, however, distinguish between the various mechanisms by which spin changes calibration.

Balancing

Before spin testing, the bearing was dynamically balanced. Small displacements of the rotating-element mass center from the spin axis cause large sinusoidal loads that increase with the square of the spin rate. A two-plane balancer was used to measure the mass distribution errors, which result from material inhomogeneity, variations in tapped thread depths, and other machining imperfections. Corrections were made by grinding edges of the calibration body and ends of screws. The entire rotating assembly has a mass of 3.5 kg (8.3 kg with calibration body) and was balanced to within 0.8 g · cm.

Spin Test Procedure

The method shown in Fig. 7 was adopted to determine spin effects. Here, gravity is used as the source of the load. The calibration rig frame permits the bearing to be mounted with its axis either horizontal or vertical. In the horizontal configuration, the bearing can also be rotated so that the lift sensors are horizontal. Thus, gravity can in essence apply normal, axial, or side forces to the calibration body.

When one of the three forces is being applied, the others are zero. Thus, two load points can be obtained in each of the three directions: one when gravity applies a finite load and one when gravity applies no load. On the assumption that the calibrations are linear, the two-point measurements permit determination of the calibration line, though admittedly with less accuracy than if many points were taken. However, these load measurements can be made at several spin rates. Thus, the effect of spin rate on calibration offset and slope can be measured.

As shown in Fig. 8, it is not necessary to know the two loads used to determine the effect of speed on slope, nor is it even necessary to know their difference. It is only necessary to ensure that they are the same at each speed. One load can be designated the zero load L_0, the other as L_1. The voltages V_0 and V_1 corresponding to the two loads are measured at each speed and the slope comparison can be calculated:

$$\frac{\text{slope}_\omega}{\text{slope}_0} = \frac{(V_{1,\omega} - V_{0,\omega})/(L_1 - L_0)}{(V_{1,0} - V_{0,0})/(L_1 - L_0)} = \frac{V_{1,\omega} - V_{0,\omega}}{V_{1,0} - V_{0,0}} \quad (1)$$

The ratio of slope at a given speed ω to that at zero speed (designated by the zero subscript) can be determined solely from the voltages measured.

The center of mass for the calibration body is not colocated with the load center for the balance. The gravitational loads are, thus, not pure forces, but contain moments about the bearing center. However, the speed sensitivity correction is applied to each sensor, not to each load axis. Thus, the loads need not be pure in any one load component, as long as two load points are obtained for each sensor.

To make the measurement, the bearing is spun at each preselected speed. The signals from the sensors are measured and recorded by a data acquisition computer. Samples are acquired at 10 kHz for 1 s. This results in recording 10 cycles at 600 rpm and 330 cycles at 20,000 rpm.

Once the motor was brought to the proper speed, the motor drive was disabled. The current stopped flowing, but the motor continued to coast. The time constant for deceleration is 350 s, so that the 1-s acquisition could be accomplished with a speed loss of less than 0.2%. The absence of current eliminates the induction of noise in the sensor wires.

The sensor signals are a combination of the effects of angle and the sinusoidal load produced by the residual mass imperfections remaining after the dynamic balancing is completed. The mass and angle effects may not be oriented identically. Because the mass effects cannot be measured precisely and then removed from the signals, the average values of the signals over many cycles are used for the spin sensitivity calculations.

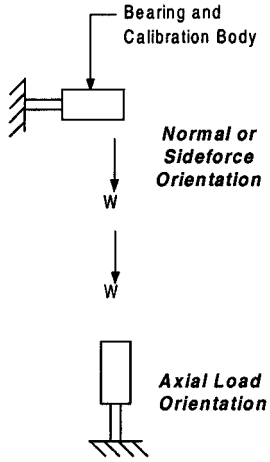

Fig. 7 Experiment to quantify spin rate effects.

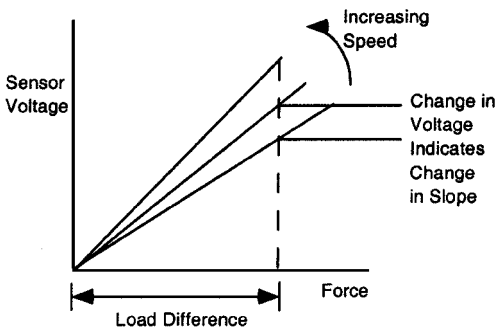

Fig. 8 Measurement at two loads is used to determine effects on line slope.

Results

Static Calibration

Figure 9 shows how sensors respond to varying normal and thrust loads. All points were taken with the bearing at the same rotation angle. Two important characteristics are visible.

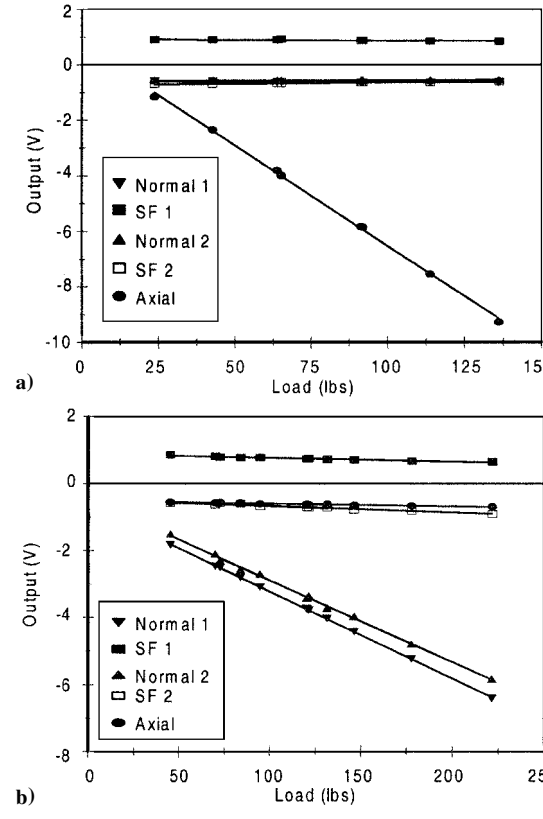

Fig. 9 Typical pressure sensor response to static loads.

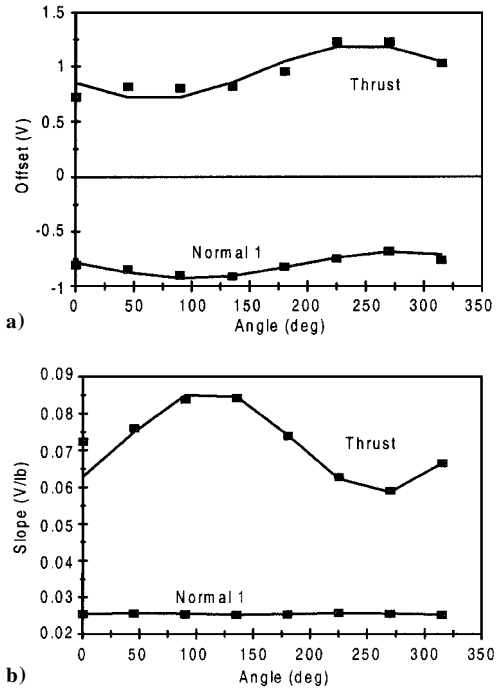

Fig. 10 Variation of a) pressure sensor offset and b) load sensitivity with angle.

First, the response of off-axis sensors is very small. For example, none of the journal sensors respond to the axial load. Similarly, the sideforce and thrust sensors show minimal response to the normal force.

Second, sensors respond nearly linearly to a load in their principal direction. Each response is characterized by a slope and an offset. The maximum deviation from the best fit line gives an estimate of the combined repeatability and linearity error. The errors are typically less than 0.5% full scale (f.s.)for lift and sideforce sensors and less than 1% f.s. for the thrust sensor.

The linearity error can be improved using higher-order fits. However, because the calibration must be applied at high frequencies (2 kHz) a linear calibration model has been adopted. The remaining errors can be attributed in part to limits on the device and the calibration rig. Some error occurs because the bearing mount deflects as load increases. Other sources include mechanical play and imprecise alignment of the cylinders with the bearing. These are artifacts of this particular calibration rig. It may be possible to produce more precise calibrations in other facilities.

Figure 10 shows how the offset and sensitivity of two sensors vary with rotor angular position. Two trends are evident. First, the journal bearing sensors, as evidenced by the normal 1 sensor, are less affected by angle than the thrust sensor. Second, all of the data presented in these two plots indicate a one-per-revolution variation. Thus, most of the variation can be accommodated by a single-sinusoid fit.

Variations in the journal bearing sensor slope are less than 1% and variations in offset are less than 3% f.s. over one revolution. For the thrust bearing, however, the variations are as large as 20% for slope and 10% f.s. for offset. The best fit sinusoid, shown in each plot, can approximate the thrust calibration parameters to within 1% f.s. and the journal sensor parameters to within 0.3% f.s., with the obvious exception of thrust at 0 deg.

Spin Testing Results

Spin tests reveal several important facts concerning the dynamic performance of the 1-DOF balance. The sensors are able to respond to variations at least as fast as 330 Hz, which corresponds to a spin rate of 20,000 rpm.

Based on the amplitudes of the signals, the bearing exhibited resonances at 130 and 260 Hz without the calibration body. These frequencies depend on the mass of the spinning body. We do not have dynamic bending data for the outer element, and so the bending modes could not be correlated with the measured resonant modes.

In the reduction of spin test data, the thrust and vertical sensor slopes were computed from the difference in the signals from a thrust load orientation and a lift load orientation. Horizontal sensor slopes are computed from the difference between a lift and a sideforce orientation. Variations in slope over the spin range were fairly small. The lift slope changes about 2% over the entire spin range, whereas the thrust slope changes about 6%. The speed effects can be approximated with a second-order curve to within 0.5% for the journal sensors and 1.2% for the thrust sensors.

Conclusions

This paper has described calibration measurements made on a 1-DOF air bearing balance. In particular, it explored the effects of rotor angle and bearing spin rate on calibration parameters. The following quantitative conclusions about calibration can be drawn from the measurements:

1) At a fixed angle, the response of the sensors is linear to within 0.5% f.s. for radial loads and 1% f.s. for thrust.

2) Calibration is a strong function of rotor angle, with slope variations of ±3% for radial load calibration and ±20% for thrust loads.

3) The angle effects can be fit with single sinusoids to within 1% for thrust and 0.3% for all other loads.

4) Over the entire spin rate range (0–20,000 rpm) the sensitivity parameters change by as much as 6%.

5) A second-order fit of the speed data matches to within 1.2% for thrust and 0.5% for other loads.

Acknowledgments

This work is sponsored by the Arnold Engineering Development Center (AEDC), Arnold Air Force Base, Tennessee, under the supervision of Ronald Bishel. The authors thank Edward Marquart of Sverdrup (AEDC) for his extensive input to and support of this work. They are also grateful for the support of the Physical Sciences, Inc., air bearing project team: Joseph Ziehler, Michael Miller, Keith McManus, Mark Allen, Joy Stafford-Evans, Henry Murphy, and Jan Polex.

References

[1]Marquart, E., and Ratliff, C., "Potential Test Technique: Virtual Flight Testing," AIAA Paper 95-3472, Aug. 1995.

[2]Burt, G. E., "Design of a Wind Tunnel Roll Damping Balance Incorporating Externally Pressurized Gas Bearings Operating at Large Film Reynolds Numbers," Arnold Engineering Development Center Rept. AEDC-TR-69-204, Arnold AFB, TN, Oct. 1969.

[3]Roblee, J. W., "Design of Externally Pressurized Gas Bearings for Dynamic Applications," Ph.D. Dissertation, Dept. of Engineering, Univ. of California, Berkeley, CA, May 1985.

[4]Gross, W. A., *Gas Film Bearings*, Wiley, New York, 1962.

[5]Hamrock, B. J., *Fundamentals of Fluid Film Lubrication*, McGraw–Hill, New York, 1994.

[6]Blondeel, E., Snoeys, R., and DeVrieze, L., "Dynamic Stability of Externally Pressurized Gas Bearings," *Journal of Lubrication Technology*, Vol. 102, Oct. 1980, p. 511.

[7]Bassani, R., and Piccigallo, B., *Hydrostatic Lubrication*, Elsevier, Amsterdam, 1992.

[8]Haldeman, C. W., and Weinberg, A. D., "Measurements on Rotating, Ablating Models Using an Air Bearing Balance," *AIAA Journal*, Vol. 30, No. 4, 1992, pp. 1039–1045.

[9]Magill, J., McManus, K., Miller, M., and Allen, M., "High-Bandwidth Air Bearing Balance for Dynamic Wind-Tunnel Testing," AIAA Paper 97-3648, Aug. 1997.

[10]Magill, J. C., McManus, K. R., Malonson, M. R., Ziehler, J. A., and Hinds, M. F., "Air Bearing Balance with One-Degree-of-Freedom Spin Capability," AIAA Paper 99-0944, Jan. 1999.

J. C. Hermanson
Associate Editor